

New Analysis and Design Tool for Achieving Low Variability Process Designs

J. L. Tseng and W. R. Cluett

Dept. of Chemical Engineering, University of Toronto, Toronto, Ontario, Canada M5S 3E5

W. L. Bialkowski

EnTech Control Engineering Inc., Toronto, Ontario, Canada M9B 6E5

A new process analysis and design tool was developed. The analysis tool consists of a systematic algorithm for analyzing a block diagram representation of a process flowsheet and identifying different paths between a given input and output variable. Transfer function representations of different paths are calculated to determine the contribution of each path to the overall attenuation characteristics of the process. To improve these attenuation characteristics, the paths that contribute the most to the overall variability must be identified and addressed. The design tool consists of a set of guidelines that the engineer can use to develop alternate process designs or control strategies to eliminate these identified paths, reduce their contribution to overall variability, or negate their effects by adding new paths. Although the ingenuity of the design engineer is critical, this tool provides the engineer with a means to identify problems in a process design, to help develop design alternatives, and a quantitative basis for comparing and evaluating these alternatives. This new tool was applied to a standard design for a stock preparation system in a pulp and paper mill.

Introduction

In order for a company to sell a product in a competitive market, it must meet the demands of the consumer in a cost-effective way. One of these demands is that product variability must be kept to a minimum (Downs and Doss, 1991). There are many sources of variability within a manufacturing process. Some of these sources can be eliminated through proper equipment maintenance. For example, bad control valves that exhibit limit cycle behavior and act as point sources of variability can be replaced. On the other hand, some sources of variability are unavoidable. Physical and chemical properties of raw materials will undoubtedly vary due to their source and storage conditions, or may depend on how the material was processed upstream of a particular unit. Once this variability is present, one of the roles of the downstream process is to reduce this variability as much as possible in order to achieve a uniform, quality product. The extent of attenuation that can be achieved by a given process depends on two main factors. First, the selection of a particular control strategy

and controller tuning will certainly have an impact on the attenuation characteristics of the process. This factor has historically been viewed by process engineers as the primary means to solve variability problems. However, the second and perhaps most important factor is the process design itself. For instance, a process design that unnecessarily contributes to final product variability may represent a loss of attenuation that cannot be recovered by even the most sophisticated control strategy.

Literature

In the past, various controllability and resiliency measures have been used to evaluate and compare alternative process designs and control strategies. Controllability refers to the ease with which a plant can maintain operation at a steady operating point. Common controllability measures include the relative gain array (RGA) (Bristol, 1966) and condition number. Resiliency refers to the degree to which a process can meet design objectives despite external disturbances and un-

Correspondence concerning this article should be addressed to W. R. Cluett.

certainties in design parameters. Common resiliency measures include the relative disturbance gain (RDG) (Stanley et al., 1985), the disturbance condition number (DCN) (Skogestad and Morari, 1987), and the disturbance cost (DC) (Lewin, 1991). Both of these types of measures are effective for comparing and screening different designs and/or control strategies. However, these measures provide little guidance to the design engineer in terms of how to conceive of alternate designs that are superior to an existing design.

Objectives and methodology

The first objective is to develop an algorithm that systematically analyzes a block diagram representation of a process, identifies all paths that exist between a given input and output variable pair, and determines the contribution each path makes to the overall attenuation characteristics of the process. By focusing on the paths that contribute the most to the overall variability, a second objective is to develop design guidelines for formulating alternative process designs and/or control strategies that result in better overall attenuation characteristics. Although the actual design changes must be conceived by the engineer, it is expected that this analysis and design tool will provide a means to identify problematic areas in a given process design, guidance with respect to the development of design alternatives, and a quantitative basis for comparing and evaluating these alternatives.

The most direct way to measure how much a process will reduce variability between two variables is to determine the process frequency response relating these two variables. For example, if the input signal is sinusoidal and the process is assumed to be linear, the resulting output signal will also be sinusoidal with the same frequency as the input signal, but typically with a different amplitude and phase. An amplitude ratio plot shows the ratio of the output sinusoid amplitude to the input sinusoid amplitude as a function of frequency. For a more general input consisting of many frequency components, the amplitude ratio plot conveys the degree to which each of these components will be attenuated by the process. Therefore, the area under the amplitude ratio plot can be used as a quantitative measure of the amount of variability that is transmitted from the input to the output within a given frequency range. Characteristics of the amplitude ratio plot that influence the area under the plot are its peak value, as well as its asymptotic slopes.

Determining the frequency response of a process can be accomplished experimentally by injecting sinusoids in the input variable and then measuring the amplitude of the resulting sinusoids in the output variable. Other types of input signals can be used (such as a pseudo random binary signal) along with spectral analysis techniques to estimate the frequency response (Ljung, 1987). However, the results of these methods would not indicate to the engineer how to alter the process design to improve its attenuation characteristics. This requires a better understanding of the process and how its structural design affects its overall frequency response characteristics. To acquire this understanding, a detailed analysis of how individual units are interconnected within the process flowsheet needs to be performed and the impact these interconnections have on the dynamic behavior of the overall process must be studied.

All chemical processes are governed by mass, energy and momentum balances which means they can be described by a set of nonlinear differential and algebraic equations. However, to achieve the stated objectives, the analysis in this article will be based on linear systems theory because this theory is well developed and because it is difficult to obtain general results for nonlinear systems (Morud and Skogestad, 1996). To derive linear models, a high fidelity nonlinear model of the process will be developed first followed by making some reasonable simplifying assumptions and linearizing the nonlinear equations about an operating point. Although this linearized model will only closely approximate the nonlinear system behavior near the point of linearization, the linearized model enables the systematic development of transfer function relationships. Frequency responses can then be calculated directly from these transfer functions for any desired frequency range. Validation of the linearized model can be done by comparing the frequency response of the linearized model to frequency responses obtained by injecting sinusoids into the high fidelity nonlinear model.

Development of Analysis and Design Tool

Transfer function development: Mason's rule

The development of a transfer function relationship between a particular input and output variable pair requires a block diagram representation of the entire system. Once the block diagram representation is created, transfer function development between any two variables within the system can be done using Mason's loop rule (Mason, 1956), given by

$$G_{ij} = \frac{\sum_k p_{ijk} \Delta_{ijk}}{\Delta} \quad (1)$$

where

G_{ij} = transfer function relationship between an input variable x_i and output variable x_j

p_{ijk} = k th forward path between x_i and x_j

Δ_{ijk} = cofactor of the forward path p_{ijk}

Δ = determinant of the entire block diagram.

The determinant Δ is given by $\Delta = 1 - (\text{sum of all different loops}) + (\text{sum of all combinations of two nontouching loops}) - (\text{sum of all combinations of three nontouching loops}) + \dots$

Nontouching loops are defined as loops that do not share any common blocks or summation nodes in the block diagram representation. The cofactor Δ_{ijk} is the determinant of the system with the loops that touch forward path p_{ijk} set equal to zero. Note that this definition of the determinant assumes that the signs on all summing junctions within the block diagram are positive.

Example of Mason's Rule (Dorf, 1980). In Figure 1, the forward paths between $x_1(s)$ and $x_2(s)$ are:

$$p_{12_1} = G_1(s)G_2(s)G_3(s)G_4(s),$$

$$p_{12_2} = G_5(s)G_6(s)G_7(s)G_8(s)$$

The loops of the process flowsheet are:

$$L_1 = G_2(s)H_2(s), \quad L_2 = G_3(s)H_3(s),$$

$$L_3 = G_6(s)H_6(s), \quad L_4 = G_7(s)H_7(s)$$

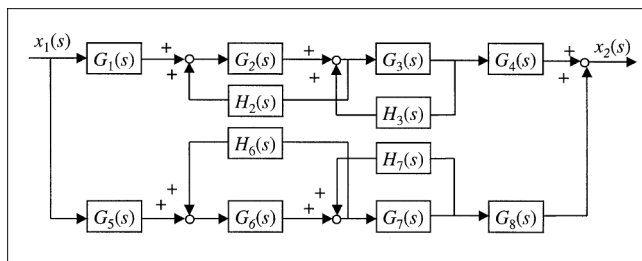


Figure 1. Block diagram for Dorf example.

Loops L_1 and L_2 touch since they share a common summation node between $G_2(s)$ and $G_3(s)$. Similarly, Loops L_3 and L_4 share the summation node between $G_6(s)$ and $G_7(s)$. Loops L_1 and L_2 do not touch loops L_3 and L_4 . The determinant is then:

$$\Delta = 1 - (L_1 + L_2 + L_3 + L_4) + (L_1 L_3 + L_1 L_4 + L_2 L_3 + L_2 L_4)$$

Loops L_1 and L_2 touch the forward path p_{12_1} . Thus, the cofactor for p_{12_1} is the determinant Δ with $L_1 = L_2 = 0$

$$\Delta_{12_1} = 1 - (L_3 + L_4)$$

Loops L_3 and L_4 touch the forward path p_{12_2} . Thus the cofactor for p_{12_2} is the determinant Δ with L_3 and $L_4 = 0$

$$\Delta_{12_2} = 1 - (L_1 + L_2)$$

The overall transfer function relationship between $x_1(s)$ and $x_2(s)$ is then

$$\begin{aligned} G_{12}(s) &= \frac{x_2(s)}{x_1(s)} = \frac{p_{12_1} \Delta_{12_1}}{\Delta} + \frac{p_{12_2} \Delta_{12_2}}{\Delta} \\ &= \frac{G_1(s)G_2(s)G_3(s)G_4(s)(1 - (L_3 + L_4))}{1 - (L_1 + L_2 + L_3 + L_4) + (L_1 L_3 + L_1 L_4 + L_2 L_3 + L_2 L_4)} \\ &\quad + \frac{G_5(s)G_6(s)G_7(s)G_8(s)(1 - (L_1 + L_2))}{1 - (L_1 + L_2 + L_3 + L_4) + (L_1 L_3 + L_1 L_4 + L_2 L_3 + L_2 L_4)} \end{aligned} \quad (2)$$

Further interpretations of Mason's rule

Defining the overall path term P_{ijk} as

$$P_{ijk} = \frac{p_{ijk} \Delta_{ijk}}{\Delta} \quad (3)$$

the overall transfer function G_{ij} can then be expressed as a sum of the overall path terms P_{ijk}

$$G_{ij} = \sum_k P_{ijk} \quad (4)$$

In a block diagram representation, G_{ij} would be equivalent

to all of the overall path terms P_{ijk} , connected in parallel, as shown in Figure 2.

This interpretation of Mason's Rule allows the decomposition of a transfer function relationship between two variables into a set of parallel path terms. This decomposition is only meaningful if there actually exists several parallel interconnections (that is, direct forward paths p_{ijk}) within the process flowsheet. Most chemical processes do involve parallel interconnections, whether they appear as external or internal connections (Morud and Skogestad, 1996). External connections refer to interconnections that exist between individual processing units. External parallel interconnections arise in process designs naturally due to piping. They also occur when feedforward control systems are used. Internal connections refer to the coupling of state variables such as temperature, stream composition, and pressure. These variables are coupled through energy, mass, and momentum balances within an individual processing unit. Internal parallel interconnections can arise from certain reaction kinetics or simultaneous heat- and mass-transfer phenomena.

From a frequency domain point of view, the decomposition of a transfer function relationship between two variables into a set of parallel path terms allows decomposition of its frequency response in terms of the frequency responses of each path term. The frequency response of a transfer function $P(s)$ at a particular frequency ω has an associated amplitude $|P(j\omega)|$ and phase $\angle P(j\omega)$

$$P(j\omega) = |P(j\omega)|e^{j\angle P(j\omega)} \quad (5)$$

This amplitude and phase can be represented by a vector in two dimensions. Since the overall process transfer function is the sum of the transfer functions associated with each parallel path, the overall frequency response can be represented as the vector sum of the frequency responses of each parallel path (see Figure 3a). If one path has an amplitude that is significantly greater than the others, the overall frequency response will be very close in amplitude and phase to the dominant path, regardless of the phases of the other paths (see Figure 3b). Thus, in the context of this article, if the ampli-

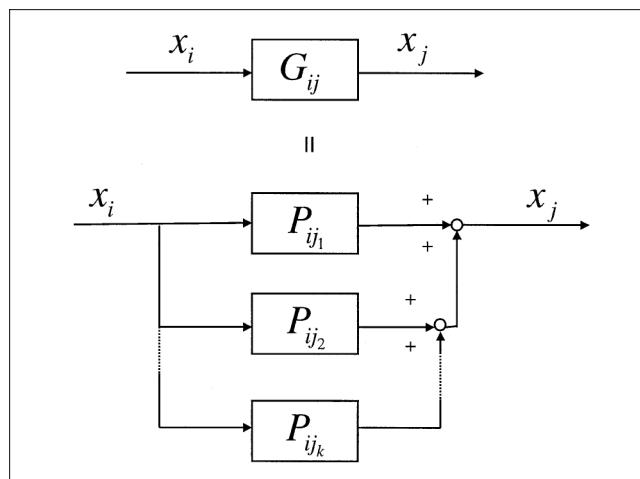


Figure 2. Parallel path block diagram representation.

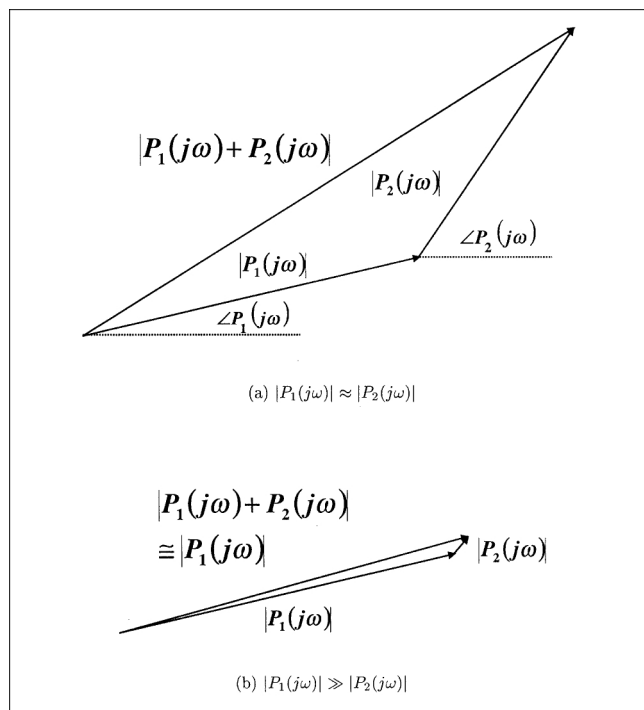


Figure 3. Sum of two transfer functions at frequency ω .

tude of the overall frequency response needs to be reduced, the dominant path must either be eliminated or reduced in amplitude. Another possibility is to add a path with a frequency response of equal amplitude and opposite phase in order to cancel the frequency response of the dominant path.

Being able to express the overall transfer function G_{ij} as the sum of individual P_{ijk} terms provides the basis for the flowsheet analysis portion of the design tool and allows one to identify and rank the contributions each path makes to the overall frequency response.

Flowsheet analysis

In order to develop an algorithm for applying Mason's loop rule to the analysis of a given process flowsheet, a software program has been written within the MATLAB/Simulink environment. To begin, a block diagram representation of the linearized process model must exist within Simulink. The algorithm consists of three stages:

Stage 1. All blocks and line connections are read from the Simulink file.

Stage 2. For a given input and output variable pair, all forward paths, their cofactors, all loops and the determinant are calculated. To calculate the forward paths and loops, the algorithm starts at the input variable and recursively follows each connection and exhaustively travels through the process flowsheet. If the output variable is encountered during the traversal, one possible forward path between the input and output variable has been found and is recorded. If a block that already has been visited is encountered again, a loop has been found and is recorded as such. In the Simulink block diagram, it is possible to specify that a group of blocks be treated as one block. This feature can be used in cases where

there is no desire to decompose a group of blocks into separate paths (such as a PI controller, which consists of two parallel paths). For the determinant, another recursive algorithm is used to determine which loops do not touch each other. Starting by comparing two loops, the algorithm checks to see whether the loops share any common blocks or summation nodes. If not, these two loops are recorded to be nontouching. The algorithm then checks to see if any loops touch these two loops. If a loop is found to not touch either of the loops, the three loops are recorded to be nontouching. The algorithm then checks if any loops touch any of these three loops, and so on. All combinations of loops are checked in this fashion. Once all combinations of nontouching loops are identified, the determinant is calculated. For the cofactor of a forward path, all loops are checked to see whether they have any blocks or summation nodes in common with that forward path. The algorithm to calculate the determinant is then used with all loops touching the forward path set equal to zero.

Stage 3. The block types (transfer function, gain, integrator and so on) and their parameters are read from the Simulink file and then the frequency response of each overall path term [that is, $P_{ijk} = (p_{ijk}\Delta_{ijk}/\Delta)$] is calculated for a given frequency range.

Various stages of the algorithm can be executed depending on the need. For example, after applying the entire algorithm once to a block diagram, if changes in block parameters are made, then only Stage 3 must be repeated to recalculate the frequency responses because the blocks, line connections, paths, loops, cofactors and determinant will not have changed. If a different input or output variable is chosen, only Stages 2 and 3 need to be executed since the blocks and line connections will not have changed.

Design guidelines

Once the block diagram has been analyzed and the frequency responses of each overall path term have been determined, any terms with frequency responses that are significantly larger in magnitude than the other responses should be dealt with first in order to improve the attenuation characteristics of the overall process. There are three main methods for approaching this problem.

Elimination. One method to address an overall path term P_{ijk} would be to eliminate it. This would require a disconnection of some sort along the direct forward path p_{ijk} . In the earlier example (Figure 1), eliminating say p_{12_2} would require eliminating either $G_5(s)$, $G_6(s)$, $G_7(s)$ or $G_8(s)$ or any of the connections between these transfer functions.

Alteration. Another method would be to alter the overall path term P_{ijk} so that its frequency response is no longer significantly higher than the responses of the other overall path terms. The most straightforward way to accomplish this would be to alter the associated direct forward path p_{ijk} . Altering the loops that touch the forward path p_{ijk} directly or indirectly via other loops would also alter the overall path term P_{ijk} . Alterations may consist of changing parameters within a block along the direct forward path. Another alternative would be to insert or extract a block to affect a variable found along the direct forward path. Again, referring to the previous example (Figure 1), if, say, P_{12_2} was the overall path term that needed to be reduced in amplitude, one could

do so by altering parameters that appear in any of the transfer functions along the forward path p_{12} [that is, parameters within $G_5(s)$, $G_6(s)$, $G_7(s)$ or $G_8(s)$]. Adding a block between, say $G_7(s)$ and $G_8(s)$ would also alter P_{12} .

Negation. A third method to deal with an overall path term would be to introduce a new path that is designed to counteract it, that is, add a path that has a frequency response with equal amplitude, but opposite phase relative to the overall path term. Feedforward control is an example of a way that attempts to do precisely this by negating a particular disturbance path.

Implementation of design guidelines

Further Considerations. Although the suggested design guidelines provide various methods for dealing with an overall path term, choosing exactly how to implement a particular method still requires careful consideration. For example, one may start by choosing to use the alteration method to reduce the amplitude of a dominant path term. Then, one must decide exactly which elements within the path to alter. Complications can arise at this stage because, in many cases, the block being altered may appear in several terms within the dominant path term and even within other overall path terms. Referring again to the example shown in Figure 1 and its overall transfer function given by Eq. 2, if the alteration method were to be used to reduce the overall path term P_{12} (assuming it to be the dominant term), one could do so by changing parameters that appeared in any of the transfer functions along the forward path p_{12} [that is, either $G_5(s)$, $G_6(s)$, $G_7(s)$ or $G_8(s)$]. However, if G_6 was altered in order to reduce the forward path, the amplitude of L_3 would also be reduced because $L_3 = G_6H_6$. Since L_3 appears in the denominator of P_{12} , reducing G_6 may increase or decrease the overall amplitude of P_{12} , depending on the amplitudes and phases of the other terms in P_{12} .

In the same way that only by eliminating dominant path terms can the overall amplitude ratio be significantly decreased, only by eliminating dominant terms in the determinant (Δ) can the amplitude of the determinant be decreased causing the overall amplitude ratio to increase (an amplitude ratio plot of all denominator terms can be used to identify which terms are dominant). Therefore, in order to ensure that design changes will reduce the overall amplitude ratio, any changes should avoid reducing the amplitude of dominant denominator terms.

Levels of Representation. The ultimate goal of the proposed analysis tool and design guidelines is to aid the engineer in developing alternate designs, starting from a given base case process design, with the objective being to improve its variability attenuation characteristics. For a given process design, there are three levels of representations that can be developed. The first level is the process flowsheet representation. The second level is a high fidelity mathematical model representation of the process. The third level is a linear block diagram representation of the process developed by linearizing the high fidelity model. It is at this third level that the proposed analysis tool is used, and the above design guidelines of eliminating, altering, or negating a variability path are applied. However, since it is at level one (the process flowsheet) that the actual process design changes need to be

implemented, changes at level three (linear block diagram) must be translated into appropriate changes at level one.

Examining the forward paths and loops of the block diagram (level three) shows that they consist of sequences of transfer functions. Each transfer function in turn represents a relationship between two variables. By identifying each transfer function relationship, the forward paths can be traced from variable to variable in the block diagram. These same variables, however, also exist in the process flowsheet (level one). Therefore, the forward paths and loops can also then be traced from variable to variable on the process flowsheet, yielding a connection between the level one and level three representations. Knowing the details of this connection can help generate ideas on how to deal with a particular forward path, such as whether it is feasible and/or appropriate to eliminate or alter a particular forward path and, if so, where within the forward path it is feasible to do so. Also, once new design alternatives have been developed, changes in the process flowsheet can be readily translated into changes in the block diagram representation. The analysis tool can then be applied to the block diagram representations of the new designs in order to compare their frequency response characteristics to the base case original design.

Case Study: Stock Preparation System

To illustrate the proposed analysis and design tool, a case study will be performed on a stock preparation system, which is a very common process area in a pulp and paper mill (see Figure 4). This process receives pulp stock from the wood chip refining stage and reduces pulp consistency (weight fraction of dry pulp) for the bleaching and paper making stages. For this process, any variability in the pulp consistency leaving the stock preparation area would have a direct effect on paper quality with high variability leading to paper products with nonuniform thickness and strength. Paper products such as cardboard boxes with uneven properties can be defective and collapse, while newsprint with nonuniform properties can cause paper breaks in the pressrooms. In a highly competitive market, the cost of product variability is quite high (Bialkowski, 1995) and can result in a pulp mill being driven out of business.

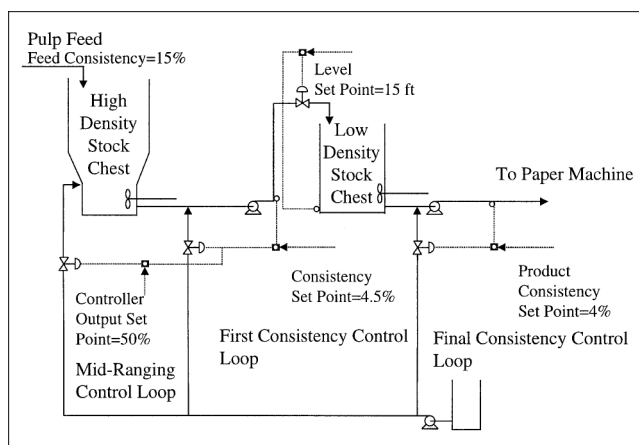


Figure 4. Process flowsheet of the stock preparation system.

Process model description

The stock feed at 500 MTD enters the high density (HD) stock chest at 15% consistency and is reduced to 5% in the bottom of the HD chest. After the HD chest, the stock consistency is reduced by another 0.5% before entering the low density (LD) stock chest. Both chests have a volume of 4,000 ft³. Following the LD chest, the consistency is again reduced by 0.5% bringing the final consistency down to 4%. Consistency is controlled after the HD chest by manipulating the minor dilution water flow. After the LD chest, the final dilution water flow is manipulated to control the final product consistency. All dilution streams share a common dilution header. Both consistency control loops have transmitters mounted within 5 s of the dilution point, and both loops are Lambda Tuned (Sell, 1995) to a closed-loop time constant of 15 s. A mid-ranging controller complements the consistency control loop following the HD chest by controlling the minor dilution water valve position using the major dilution water stream. The mid-ranging control loop is also Lambda Tuned to a closed-loop time constant of 900 s.

The high density stock chest is modeled as a plug-flow reactor (PFR) followed by a continuously stirred tank reactor (CSTR). The PFR volume is 60% of the total high density chest volume. The low density stock chest is modeled as a CSTR (perfect mixing). Perfect, instantaneous mixing is assumed where dilution water is added to the stock after the HD and LD chests. The dilution water pump is assumed to have a linear droop operating at 40 psi (280 kPa) at nominal operating conditions and increasing to 50 psi (340 kPa) at zero dilution water flow. The dilution water flow rate/header pressure system is modeled to be a first-order process with a 0.25 s time constant. Friction losses in the dilution water system are neglected. Level is controlled to 15 ft (4.6 m) in the LD chest while the level in the HD chest is assumed to be constant at 15 ft. The LD chest level controller is Lambda Tuned to a closed-loop time constant equal to the residence time of the LD chest (880 s). Changes in dilution water flow rates are assumed to have a negligible effect on tank residence times. Both consistency control valves are assumed to behave as first-order systems with a time constant of three seconds. The mid-ranging control valve dynamics are neglected. No nonlinear valve characteristics are modeled. A list of process modeling equations can be found in the Appendix.

To obtain the block diagram representation, the consistency mass balance equations at the dilution water mixing points are linearized using a Taylor series expansion. The valve/pressure-drop/flow relationships are also linearized. With the block diagram representation, the flowsheet analysis tool is used to identify the various paths and loops between the feed and product consistency. The amplitude frequency response is then calculated for each overall path term. These frequency responses provide a basis for comparing the attenuation characteristics of each overall path and determining whether there are any paths that negatively impact the attenuation characteristics of the process design. The amplitude frequency responses are also calculated for each term in the determinant. These responses provide a basis for determining which areas within the process to avoid altering while attempting to address a particular forward path. Subse-

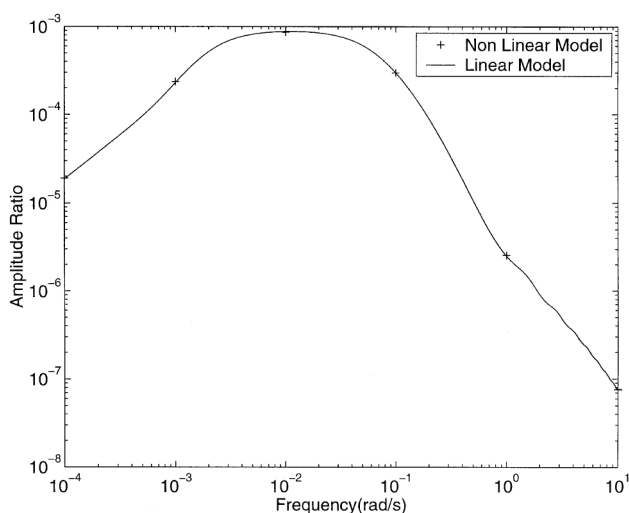


Figure 5. Comparison of linear frequency response and nonlinear model responses for feed consistency to product consistency.

quently, the design guidelines are applied in order to develop alternate process designs that improve the overall attenuation characteristics of the process between feed and product consistency.

The linear model is validated by comparing the frequency response between feed and product consistency with discrete frequency responses obtained by injecting sinusoids into the feed consistency of the nonlinear model and measuring the amplitude and phase shift of the product consistency. For the base case process design described above, using an input amplitude of 1% consistency, the linear response matches the discrete, nonlinear responses (see Figure 5).

Results and discussion

Base Case Design: Common Dilution Header. The process flowsheet analysis tool identifies three forward paths between feed consistency and product consistency (see Figures 6–8). The first forward path p_1 follows the path of the stock

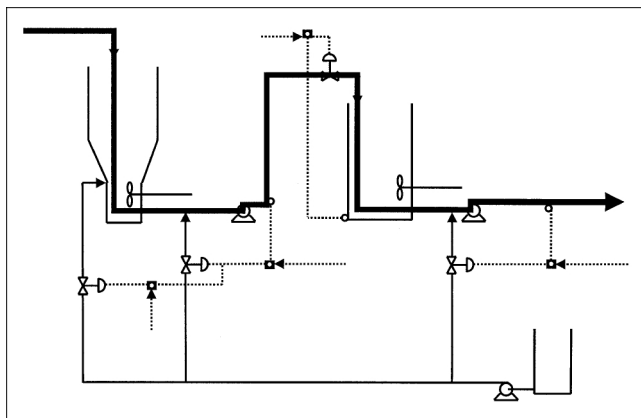


Figure 6. Forward path p_1 on process flowsheet: stock flow path.

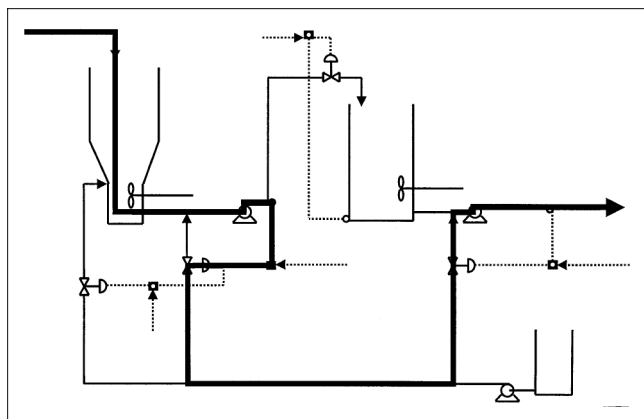


Figure 7. Forward path p_2 on process flowsheet: path through first consistency controller.

itself. This would represent the intended path for achieving variability reduction. From the feed consistency, variability passes through the HD chest to the outlet consistency of the HD chest. After the mixing point with the minor dilution stream, variability propagates to the inlet consistency entering the LD chest, passing through to the outlet consistency of the LD chest and finally to the product consistency after the final dilution mixing point. The second forward path p_2 starts off the same as p_1 , going from the feed consistency, through the HD chest to the HD outlet consistency and past the first dilution mixing point to the LD inlet consistency. Variations in consistency after this dilution mixing point, however, are detected by the consistency sensor that sends a signal to the first consistency controller. This controller varies the control valve regulating the minor dilution flow rate, which in turn causes variations in header pressure. Since all dilution streams share a common header, all dilution stream flow rates are subsequently affected by the variation in any one stream flow rate. Thus, variations from the header pressure cause variations in the final dilution stream flow, which then cause variations in product consistency via the last dilution mixing point. The third forward path p_3 is similar to p_2 . However, after the first consistency controller, a signal is also sent to the

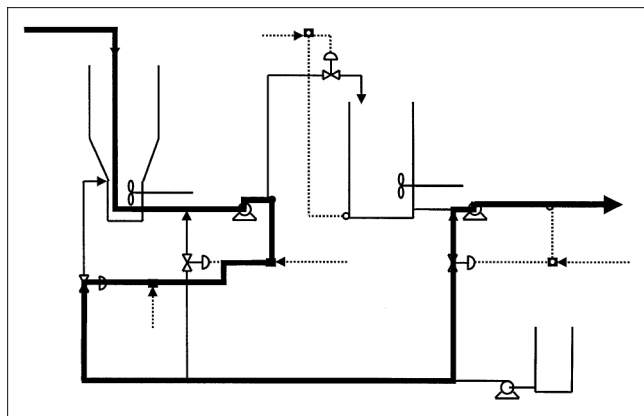


Figure 8. Forward path p_3 on process flowsheet: path through mid-ranging controller.

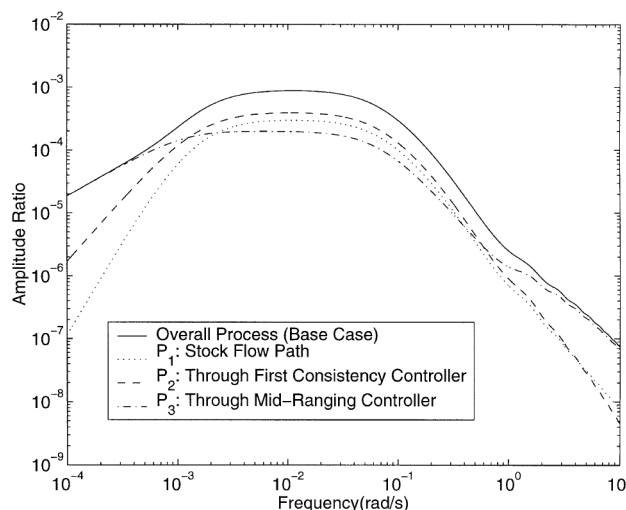


Figure 9. Frequency response for feed consistency to product consistency for the base case design.

mid-ranging controller, which varies the control valve regulating the major dilution flow rate. This flow rate variation affects the header pressure which in turn affects the other dilution flow rates via the common header. The variations in the final dilution stream flow cause variations in the final product consistency.

The process flowsheet analysis tool also identifies a total of ten loops within the process. After determining which loops do and do not touch each other, the determinant is given by

$$\begin{aligned} \Delta = & 1 - (L_1 + L_2 + L_3 + L_4 + L_5 + L_6 + L_7 + L_8 + L_9 + L_{10}) \\ & + (L_1L_2 + L_1L_3 + L_1L_5 + L_2L_4 + L_2L_5 + L_2L_6 \\ & + L_2L_7 + L_2L_8 + L_3L_7 + L_6L_7) \\ & - (L_1L_2L_5 + L_2L_6L_7) \end{aligned} \quad (6)$$

The location of these loops within the process flowsheet will be identified as needed below.

Forward Path Analysis. Frequency response plots of the overall paths terms (that is, $P_k = p_k \Delta_k / \Delta$, $k = 1, 2, 3$) in Figure 9 shows that all overall path terms have frequency responses with similar gains between 2×10^{-3} and 0.5 rad/s. However, for frequencies less than 2×10^{-3} rad/s and frequencies greater than 0.5 rad/s, the gain associated with P_3 (involving the forward path going through the first consistency controller and the mid-ranging controller) is much larger than the gains associated with P_1 and P_2 . Thus, the overall frequency response mainly takes on the attenuation characteristics of this dominant path within these frequency regions. It is also worth noting that, for frequencies lower than 0.5 rad/s, the gain of P_2 (involving the forward path going through the first consistency controller) is higher than the gain of P_1 (involving the stock flow path), especially for frequencies less than 2×10^{-3} rad/s. In fact, the responses for P_2 and P_3 have lower asymptotic slopes in the low frequency region than the response for P_1 (+20 dB/decade for P_3 , +40 dB/decade for P_2 and +60 dB/decade for P_1).

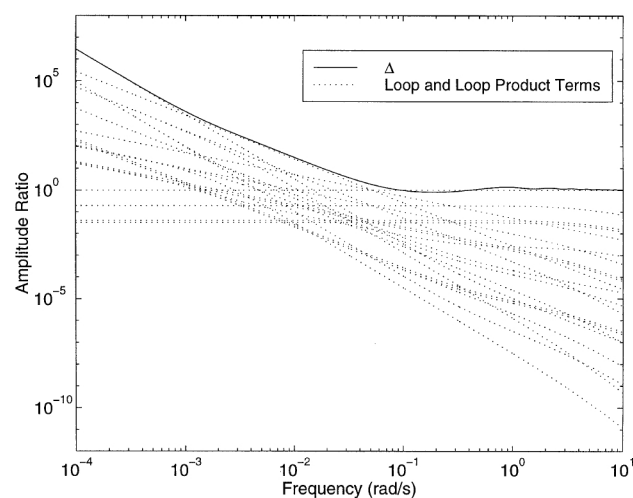
The asymptotic slopes associated with an amplitude ratio frequency response represent an important attenuation characteristic, because they significantly affect the area under the frequency response within a certain frequency range. The lower slopes in the lower frequency region of the responses for P_2 and P_3 can be attributed to the fact that both forward paths p_2 and p_3 bypass the LD chest, which acts as a low pass filter with a slope of zero in the lower frequency region. Instead, p_2 goes through a consistency controller that has a slope of -20 dB/decade in the lower frequency region while p_3 goes through both the first consistency controller and the mid-ranging controller that combine to give a -40 dB/decade slope in the lower frequency region. Subsequently, the slopes of the responses for P_2 and P_3 are reduced by 20 dB/decade and 40 dB/decade, respectively.

Since P_2 and, in particular, P_3 have significantly higher gains as compared to P_1 , any design changes to improve the attenuation characteristics of the overall process need to address these two overall path terms. In order for a design

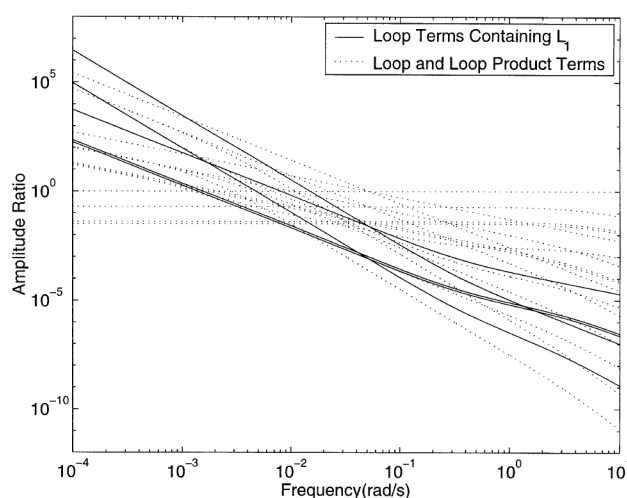
change to affect both paths, it must either affect a variable or a transfer function relationship that is common to both paths. However, the design change should also try to avoid affecting a variable or a transfer function relationship that is also common to any dominant term in the determinant.

Loop Analysis. Figure 10a shows an amplitude ratio frequency response plot of all terms in the determinant given in Eq. 6 (including the first term equal to unity), as well as the determinant itself (highlighted). This figure shows that the frequency response of the determinant is largely determined by certain dominant terms. For instance, in the high frequency region ($> 1 \times 10^{-1}$ rad/s), the dominant term is the constant unity term.

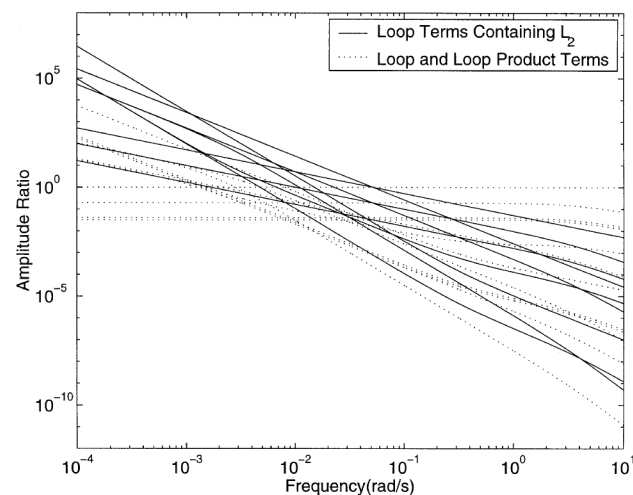
Figure 10b highlights the terms that contain L_1 , that is, L_1 , L_1L_2 , L_1L_3 , L_1L_5 and $L_1L_2L_5$. If L_1 is reduced in amplitude or even eliminated, then all terms containing L_1 would be affected. From Figure 10b, the loop terms that contain L_1 are not significant in the middle or high frequency region, but one of the terms is dominant in the low frequency region



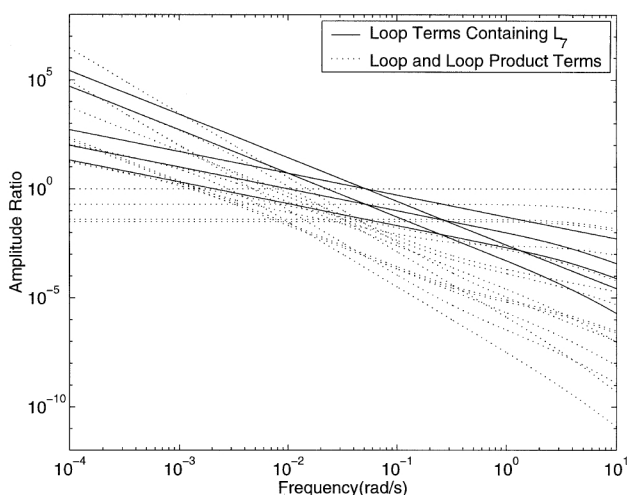
(a) Determinant



(b) Terms containing Loop 1



(c) Terms containing Loop 2



(d) Terms containing Loop 7

Figure 10. Frequency responses of loop terms in determinant.

($<1 \times 10^{-3}$ rad/s). Therefore, reducing the amplitude of L_1 would reduce the amplitude of the determinant in this frequency region which in turn may lead to a significant increase in the amplitude of the overall frequency response.

Figure 10c highlights the terms that contain L_2 and Figure 10d highlights the terms that contain L_7 . Some of the terms containing L_2 are very significant in the low and middle frequency region ($<1 \times 10^{-1}$ rad/s), while some of the L_7 terms are significant in the middle frequency range (between 1×10^{-3} and 1×10^{-1} rad/s). Similar analysis for L_3 , L_4 , L_5 , L_6 , L_8 , L_9 , and L_{10} shows that terms containing these loops are not significant in any frequency region.

Figure 11a shows Loop 1 on the process flowsheet. Consistency after the minor dilution mixing point is detected by the consistency sensor and transmitted to the first consistency controller. The actions of the consistency controller are sent to the mid-ranging controller that manipulates the major dilution stream valve, which affects the major dilution stream flow rate. This flow rate, in turn, affects the consistency in the HD chest and of the stream leaving the HD chest, which then proceeds to the minor dilution mixing point.

Figure 11b shows Loop 2 on the process flowsheet. Consistency after the final dilution mixing point is measured by a consistency sensor and transmitted to the final consistency controller. The controller manipulates the final dilution stream valve, which affects the final dilution stream flow rate. This flow rate then affects the consistency of the stream leaving the LD chest, which then proceeds to the final dilution mixing point.

Figure 11c shows Loop 7 on the process flowsheet. Consistency after the minor dilution mixing point is measured by the consistency sensor and transmitted to the first consistency controller. This controller manipulates the minor dilution stream valve, which affects the minor dilution stream flow rate. This flow rate then affects the consistency at the minor dilution mixing point.

In order to prevent the determinant from being significantly reduced in any frequency region, any design change should not only address the two significant overall paths P_2 and P_3 , but should also avoid affecting Loops 1, 2 and 7.

Shared Blocks Among Path and Loop Terms. Using the analysis tool, a comparison of Loop 1, 2 and 7 with the two forward paths associated with the dominant overall path terms P_2 and P_3 shows that there are three blocks common to both forward paths p_2 and p_3 that are not present in Loop 1, 2 or 7. They are:

- A summation block that sums the dilution stream flow rate deviations of the major dilution stream, minor dilution stream, and the final dilution stream.
- A block that represents the transfer function relationship between total dilution stream flow rate deviation and header pressure deviation, which is modeled here as a first-order transfer function with a time constant of 0.25 s.
- A gain block that represents the linearized relationship between header pressure deviation and the final dilution stream flow rate deviation.

Since these blocks are common to both forward paths and not present in the dominant loop terms, the same is true for the output variables of each of these blocks. The output variables associated with each of these three blocks are:

- The total dilution stream flow rate deviation due to devi-

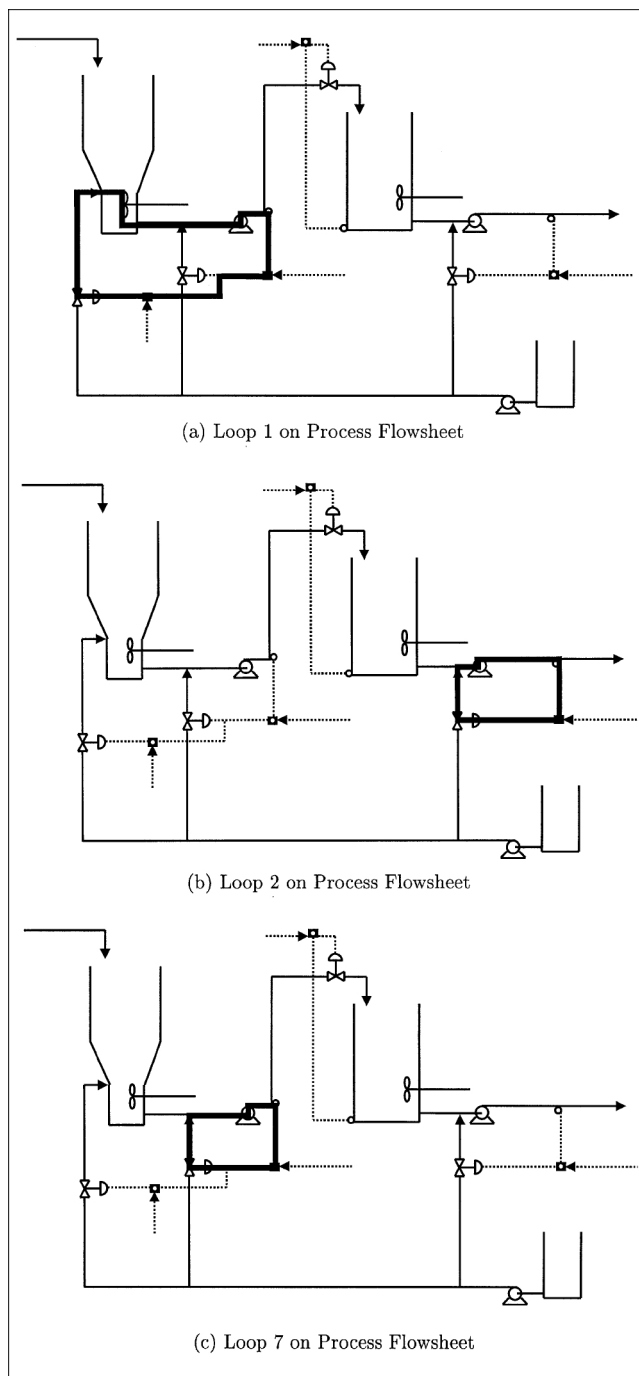


Figure 11. Process flowsheet highlighting loops 1, 2 and 7.

ations of the major dilution stream, minor dilution stream and the final dilution stream.

- Header pressure deviation due to total dilution stream flow rate deviation.
- Final dilution stream flow rate deviation due to header pressure deviation.

Thus, any design change should address at least one of these variables or the relationships represented by these blocks.

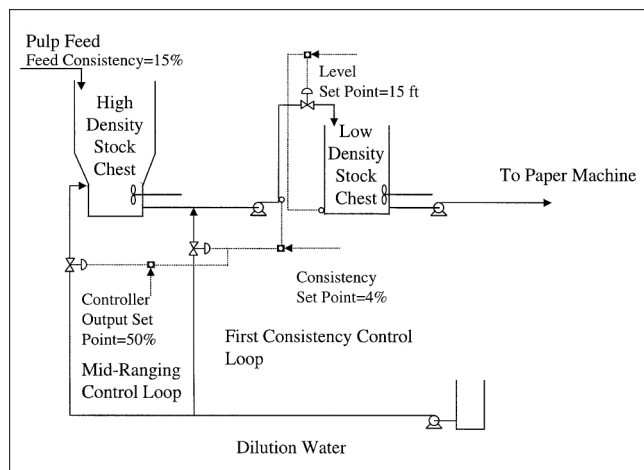


Figure 12. Process flowsheet for alternate design I.

Alternate Design I: No Dilution Water Added After the LD Stock Chest. Analysis of the base case design shows that any alternate design to improve overall attenuation between feed and product consistency requires that the overall path terms P_2 and P_3 be addressed. One possible way to deal with these terms is to apply the elimination method to their corresponding forward paths p_2 and p_3 . The path and loop analysis shows that one of the variables that is common to both forward paths but not common to any of the dominant determinant terms is the final dilution flow rate deviation due to header pressure deviation. By examining the process flowsheet, it can be seen that one simple way to eliminate final dilution stream flow rate deviations arising from header pressure deviations is to eliminate the final dilution stream along with its consistency control loop (see Figure 12). The amount of dilution water added after the HD chest can be increased in order to make up for the loss of the final dilution stream.

After performing the flowsheet analysis on this new alternate design, the analysis now shows only one forward path between the feed and product consistency, namely the path of the stock itself. However, the amplitude ratio frequency response plot of the corresponding overall path term shows that, although the forward paths that were bypassing the LD chest have been eliminated, the attenuation characteristics of this design are worse than those associated with the base case design in the low frequency region (see Figure 13). Figure 14 shows that the determinant has been significantly reduced for frequencies less than 1×10^{-1} rad/s. This, in turn, affects the frequency response of the overall path term, with the low frequency slope being +40 dB/decade as opposed to +60 dB/decade for P_1 in the base case design. As a result, the peak amplitude and area under the response of this alternate design have in fact increased when compared to the base case design.

A closer examination of the process flowsheet in Figure 12 shows that, although this alternate design eliminated final dilution flow rate deviations due to header pressure deviations, it also eliminated Loop 2 (see Figure 11b). Recall from Figure 10c that determinant terms involving Loop 2 are very significant in the low frequency region. Therefore, with Loop 2 eliminated in the alternate design, these determinant terms

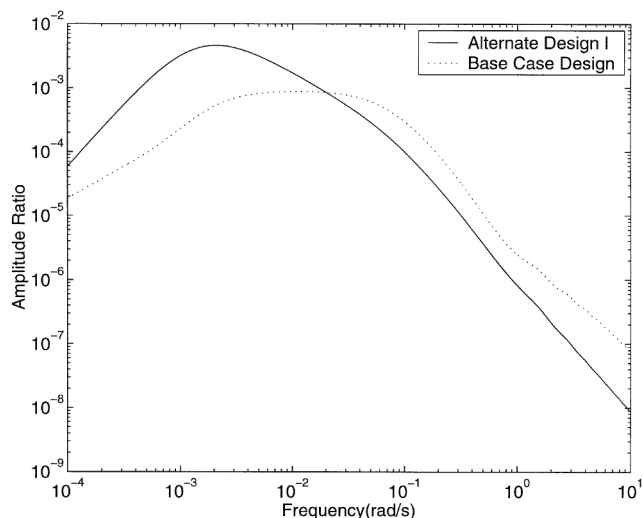


Figure 13. Frequency response for feed consistency to product consistency for alternate design I.

are eliminated, which in turn reduces the determinant in the low frequency region causing an increase in the overall frequency response.

In conclusion, although this alternate design targeted one of the variables shared by the dominant overall path terms P_2 and P_3 in the base case design, it also eliminated one of the dominant terms in the determinant, Loop 2. This resulted in an alternate design with worse attenuation characteristics than the base case design.

Alternate Design II: Final Consistency Control Loop Using a Dedicated Dilution Header. Continuing with the implementation of the elimination method on P_2 and P_3 , a better way to eliminate final dilution stream flow rate deviations arising from header pressure deviations is to disconnect the final dilution stream from the main header and use a separate dedicated pump (see Figure 15). This new pump is assumed to

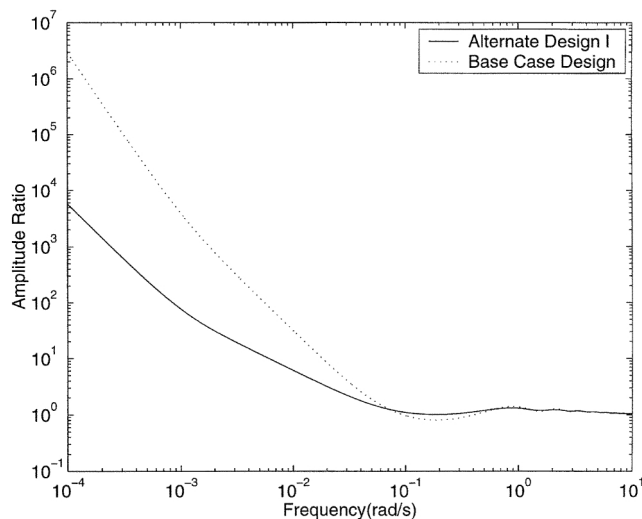


Figure 14. Frequency response of the determinant of alternate design I.

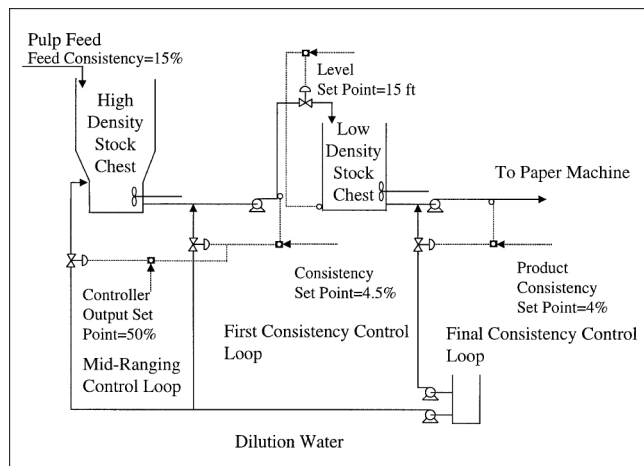


Figure 15. Process flowsheet for alternate design II.

have a linear droop operating at 40 psi at nominal operating conditions and increasing to 50 psi at zero dilution water flow.

A flowsheet analysis for this design shows that only the stock flow path itself exists as a forward path between the feed and product consistency. By using a dedicated dilution water header for the final consistency control loop, the frequency response of the determinant has not been significantly altered from the base case design (see Figure 16). As a result, the attenuation characteristics associated with this alternate design have not significantly changed from P_1 of the base case design. With the other forward paths p_2 and p_3 eliminated, the overall frequency response is now much lower than the overall response of the base case design in the low and high frequency region (see Figure 17).

Alternate Design III: Header Pressure Control. In the previous two alternate designs, the elimination method was used on overall path terms P_2 and P_3 in order to improve overall attenuation. The alteration method can also be used to im-

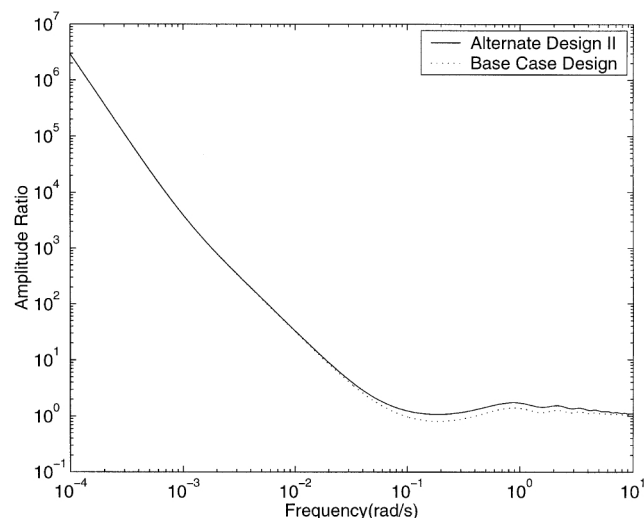


Figure 16. Frequency response of the determinant of alternate design II.

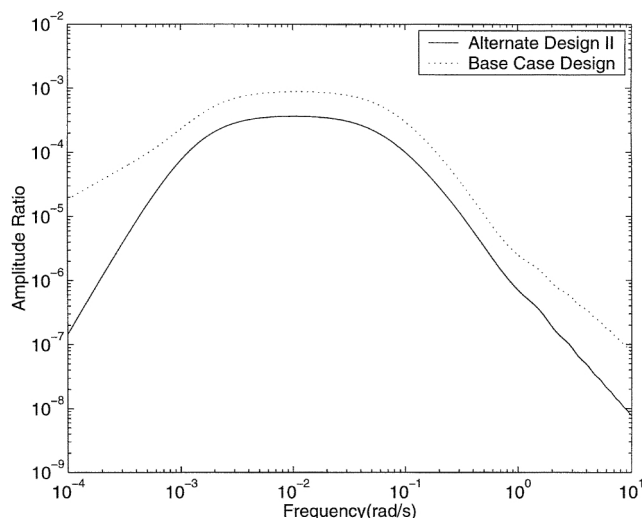


Figure 17. Frequency response for feed consistency to product consistency for alternate design II.

prove overall attenuation. The most direct way to alter P_2 and P_3 is to alter their respective forward paths p_2 and p_3 . From the earlier path and loop analysis, a variable that is common to both forward paths is the header pressure deviation. If variations in header pressure can be reduced, the gains associated with p_2 and p_3 will decrease. Looking at the process flowsheet, this can be accomplished by implementing feedback control of the header pressure. Using a variable speed pump, rotation speed is manipulated in order to control header pressure (see Figure 18). The pump is assumed to have first-order dynamics with a time constant of 0.25 s. The pressure controller is Lambda Tuned to a closed-loop time constant of 2 s.

Using the flowsheet analysis tool, the same three forward paths exist as in the base case design. However, the pressure control loop inserts a new block, that is, a control loop sensitivity function, in both forward paths p_2 and p_3 . This addition of the pressure control loop does not significantly affect the frequency response of the determinant (see Figure 19).

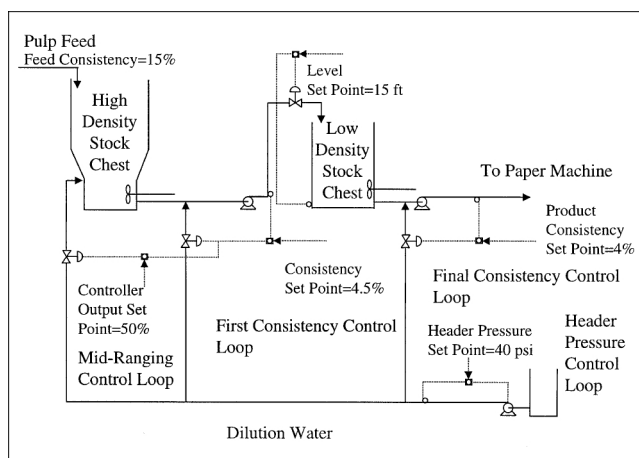


Figure 18. Process flowsheet for alternate design III.

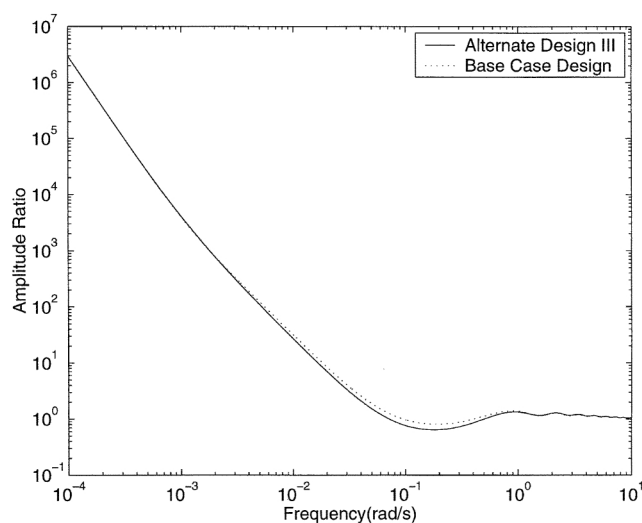


Figure 19. Frequency response of the determinant of alternate design III.

As a result, the frequency response of P_1 involving the stock flow path is relatively unchanged compared to P_1 of the base case design. With the determinant relatively unchanged, and with p_2 and p_3 altered by the sensitivity function, the attenuation characteristics of their respective overall path terms P_2 and P_3 have been dramatically affected (see Figure 20) and are now much lower than the gain of P_1 for frequencies less than 0.5 rad/s. Thus, for lower frequencies, the pressure controller has effectively eliminated interactions among all dilution streams, and the overall attenuation characteristics of the process match that of the stock flow path P_1 . For frequencies higher than 0.5 rad/s, the responses for P_2 and P_3 resemble their responses in the base case design. This is because the pressure controller is not effective beyond its bandwidth so the paths through the dilution header tend to domi-

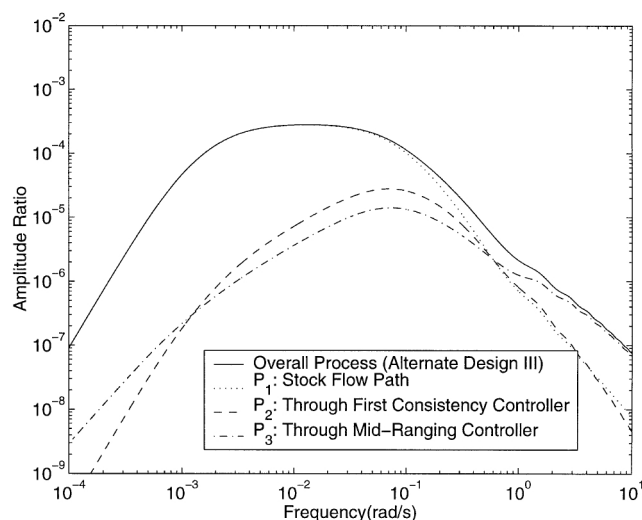


Figure 20. Frequency response for feed consistency to product consistency for alternate design III.

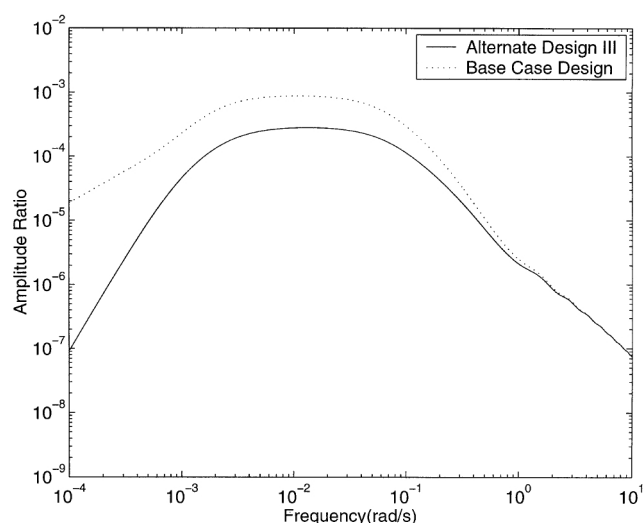


Figure 21. Frequency response for feed consistency to product consistency for alternate design III.

nate the attenuation characteristics of the overall process as they did in the base case design (see Figure 21).

Design Comparison. Figure 22 shows a comparison of the frequency responses for the base case common header design, the design with no final dilution water (I), the dedicated header design (II) and the design with pressure control (III). Table 1 shows the peak amplitudes of these frequency responses and the areas under the frequency responses above -180 dB. Among all the designs considered, the pressure control design and the dedicated header design have the best attenuation characteristics in terms of low frequency asymptotic slope, peak amplitude, and total area under the frequency response.

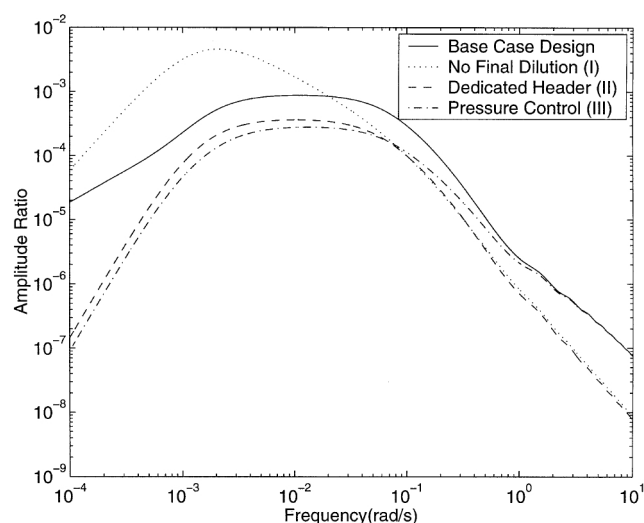


Figure 22. Frequency response for feed consistency to product consistency for base case design and alternate designs.

Table 1. Comparison of Designs

	Peak Amplitude (dB)	Area Above -180 dB 10^{-4} –10 rad/s (dB ²)
Base case: common header design	-61.2	9.41×10^3
Alt. design I: no final dilution	-46.8	9.54×10^3
Alt. design II: dedicated header	-68.8	8.10×10^3
Alt. design III: pressure control	-71.0	8.33×10^3

Conclusions

This article presents the development of a new process analysis and design tool. The tool is designed to analyze a given process flowsheet using Mason's Rule and to calculate the frequency responses of all individual parallel path terms between a given input and output variable pair which sum to form the overall frequency response. An analysis of the individual frequency responses of these path terms shows whether any particular paths dominate the overall frequency response. If so, using design guidelines presented as part of this work, a method for dealing with problematic paths can be selected (that is, elimination, alteration, or negation). By tracing each variable within each path and comparing common variables among paths, changes that are made to the block diagram representation can be related to changes in the process flowsheet. Although specific design changes must be conceived by the user, this new tool can provide valuable insight and guidance to the engineer during the process design stage. The flowsheet analysis and design tool was illustrated by application to a common process found in the pulp and paper industry, the stock preparation system.

Acknowledgments

The first two authors would like to acknowledge the Natural Sciences and Engineering Research Council of Canada for their financial support of this work. All authors would like to thank the reviewers for their helpful comments, in particular Reviewer No. 1 who pointed out to us an important issue concerning the impact of design changes on the determinant.

Notation

A = cross-sectional area of tank, m²
 C_{v1a} = major dilution stream valve coefficient, gpm/psi^{1/2}
 C_{v1} = dilution stream (after HD chest) valve coefficient, gpm/psi^{1/2}
 C_{v2} = dilution stream (after LD chest) valve coefficient, gpm/psi^{1/2}
 CSTR = continuous stirred tank reactor
 F_{feed} = total feed (dry pulp + water) mass-flow rate, kg/s
 F_{in2} = stock mass-flow rate entering LD chest, kg/s
 F_{out1} = stock mass-flow rate exiting HD chest, kg/s
 F_{out2} = stock mass-flow rate exiting LD chest, kg/s
 F_{prod} = product stock mass-flow rate, kg/s
 F_{w1a} = major dilution mass-flow rate, kg/s
 F_{w1} = dilution water (after HD chest) mass-flow rate, kg/s
 F_{w2} = dilution water (after LD chest) mass-flow rate, kg/s
 HD = high density
 k = conversion factor, (kg/s)/gpm
 K_{c_h} = level controller gain, kg/m³·s
 K_{c_m} = mid-ranging controller gain, % consistency/% valve position
 K_{c_x} = consistency controller gain, % consistency/% valve position
 K_{p_h} = process gain between inlet flow rate and level, m/kg
 K_{p_m} = process gain between major dilution valve position and consistency controller output, % valve position/% consistency
 K_{p_x} = process gain between valve position and consistency, % valve position/% consistency

g = constant of gravity, m/s²
 h = LD chest level, m
 LD = low density
 P_{max} = maximum header pressure, psi
 P_{pump} = header pressure, psi
 P_{tank} = pressure at the bottom of the 15-ft chest, psi
 PFR = plug-flow reactor
 PI = proportional integral
 V = LD chest volume, m³
 V_A = HD chest holding area volume, m³
 V_B = HD chest mixing area volume, m³
 vp_{1a} = major dilution stream valve position, % open
 vp_1 = dilution stream (after HD chest) valve position, % open
 vp_2 = dilution stream (after LD chest) valve position, % open
 x_{feed} = feed consistency, %
 x_{in2} = consistency entering LD chest, %
 x_{out1} = consistency leaving HD chest, %
 x_{out2} = consistency leaving LD chest, %
 x_{prod} = product consistency, %
 y_1 = first consistency controller output
 y_2 = second consistency controller output
 λ_x = consistency controller closed-loop time constant, s
 λ_h = level controller closed-loop time constant, s
 ρ = stock density, kg/m³
 τ_{d_h} = process delay between LD chest inlet flow rate and level, s
 τ_{d_m} = process delay between major dilution valve position and consistency controller output, s
 τ_{d_x} = process delay between valve position and consistency, s
 τ_{p_m} = residence time of mixing volume of HD chest, s
 τ_{p_p} = time constant of dilution header system, s
 τ_{p_v} = valve time constant, s
 τ_{p_x} = level controller integral time constant, s
 τ_{I_m} = mid-ranging controller integral time constant, s
 τ_{I_x} = consistency controller integral time constant, s

Literature Cited

- Bialkowski, W. L., "Design of the Low Variability Mill: But at What Operating Cost?," *The Entech Report*, **7**, 2 (1995).
 Bristol, E. H., "On a New Measure of Interaction for Multivariable Process Control," *IEEE Trans. Automatic Control*, **AC-11**, 133 (1966).
 Dorf, R. C., *Modern Control Systems*, Addison-Wesley, Reading, MA (1980).
 Downs, J. J., and J. E. Doss, "Present Status and Future Needs—A View from North American Industry," *Proc. Int. Conf. on Chemical Process Control*, Padre Island, TX, p. 53 (1991).
 Lewin, D. R., "Feedforward Design Using the Disturbance Condition Number," *Proc. IFAC Symp. on Adv. Control of Chem. Processes*, Toulouse, France, p. 203 (1991).
 Ljung, L., *System Identification: Theory for the User*, Prentice-Hall, Englewood Cliffs, NJ (1987).
 Mason, S. J., "Feedback Theory: Further Properties of Signal Flow Graphs," *Proc. IRE*, **44**, 920 (1956).
 Morud, J., and S. Skogestad, "Dynamic Behaviour of Integrated Plants," *J. Proc. Cont.*, **6**, 145 (1996).
 Sell, N. J., *Process Control Fundamentals for the Pulp and Paper Industry*, TAPPI Press, Atlanta, GA (1995).
 Skogestad, S., and M. Morari, "Effect of Disturbance Directions on Closed-Loop Performance," *Ind. Eng. Chem. Res.*, **26**, 2029 (1987).
 Stanley, G., M. Marino-Galarraga, and T. J. McAvoy, "Shortcut Operability Analysis: 1. The Relative Disturbance Gain," *Ind. Eng. Chem. Process Des. Dev.*, **24**, 1181 (1985).

Appendix: Stock Preparation Model Equations

High density stock chest

Refer to Figure A1.

Component balance around mixing volume V_B (m³)

$$x_{\text{feed}}(\text{delayed})F_{\text{feed}} - x_{\text{out1}}F_{\text{out1}} = \frac{d}{dt}(\rho V_B x_{\text{out1}})$$

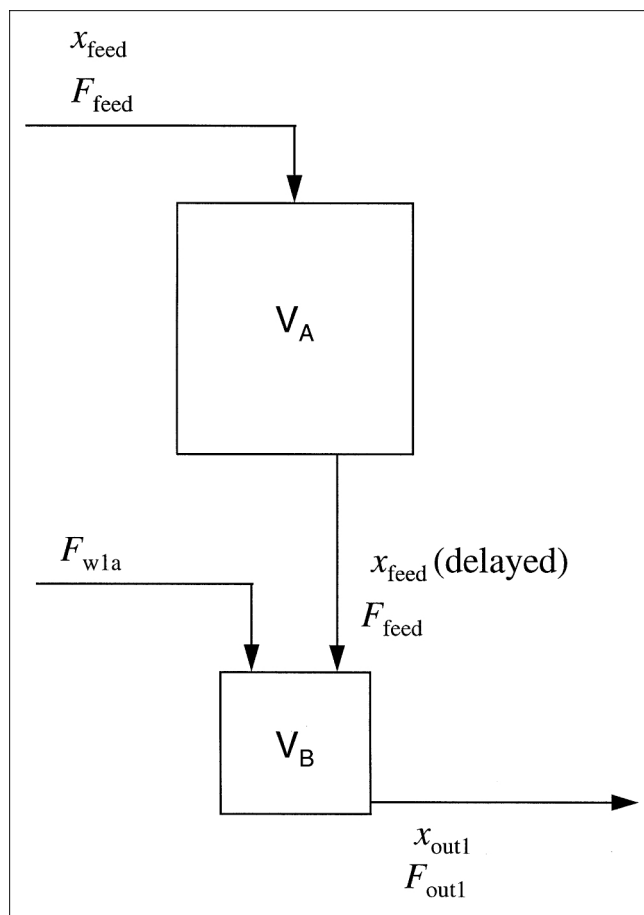


Figure A1. High density stock chest.

Overall material balance around V_B

$$F_{\text{feed}} + F_{w1a} - F_{\text{outl}} = \frac{d}{dt}(\rho V_B)$$

Overall material balance around HD chest

$$F_{\text{feed}} + F_{w1a} - F_{\text{outl}} = \frac{d}{dt}[\rho(V_A + V_B)]$$

Flow equation

$$F_{w1a} = k(vp_{1a}/100)C_{v1a}\sqrt{P_{\text{pump}} - P_{\text{tank}}}$$

The pressure at the bottom of the tank P_{tank} is given by

$$P_{\text{tank}} = \rho gh$$

Line losses were neglected. Thus, the pressure upstream of the valve is assumed to be equal to the header pressure P_{pump} (psi).

Dilution water mixing point after HD chest

Refer to Figure A2.

Changes in F_{in2} are assumed to only affect the outlet flow rate of the high density stock chest (F_{outl}) and not the minor dilution flow rate (F_{w1}) since F_{outl} is much greater than F_{w1} (an order of magnitude higher). Changes in F_{w1} are assumed to only affect F_{outl} and not F_{in2} . Thus, at this mixing point, F_{outl} is the only dependent variable.

Overall material balance

$$F_{\text{outl}} = F_{\text{in2}} - F_{w1}$$

Flow equation

$$F_{w1} = k(vp_1/100)C_{v1}\sqrt{P_{\text{pump}} - P_{\text{tank}}}$$

The consistency entering the LD chest (%), x_{in2} , will be controlled by manipulating the valve position of the minor dilution stream vp_1 . A PI controller is used with controller gain

$$K_{c_x} = \frac{\tau_{I_x}}{K_{p_x}(\lambda_x + \tau_{d_x})}$$

and integral time constant (s)

$$\tau_{I_x} = \tau_{p_x}$$

The consistency control valve is assumed to have first-order characteristics

$$vp_1'(s) = \left(\frac{1}{\tau_{p_x}s + 1} \right) y_1'(s)$$

The consistency controller output y_1 will be controlled by manipulating the valve position of the major dilution stream vp_{1a} . A PI controller is used with controller gain

$$K_{c_m} = \frac{\tau_{I_m}}{K_{p_m}(\lambda_m + \tau_{d_m})}$$

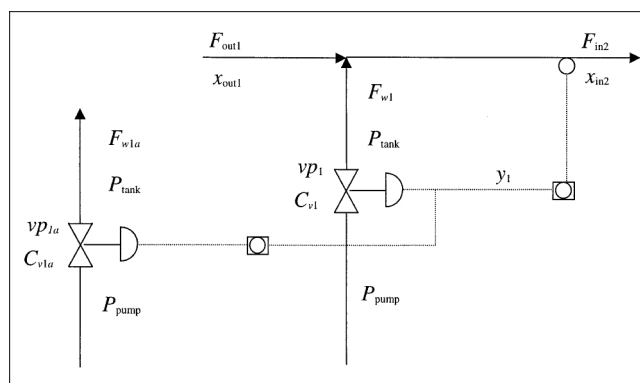


Figure A2. Dilution water mixing point after HD chest.

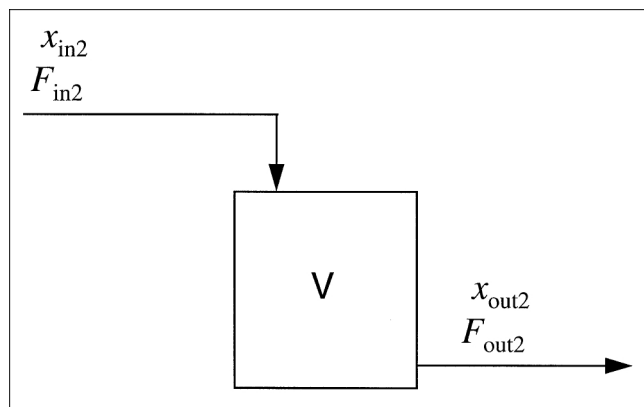


Figure A3. Low density stock chest.

and integral time constant

$$\tau_{I_m} = \tau_{p_m}$$

Low density stock chest

Refer to Figure A3.

Component balance around LD chest

$$x_{in2}F_{in2} - x_{out2}F_{out2} = \frac{d}{dt}(\rho V x_{out2})$$

Overall material balance around the LD chest

$$F_{in2} - F_{out2} = \frac{d}{dt}(\rho V)$$

Changes in F_{out2} will cause the level in the low density chest to change. The level h will be controlled by manipulating the inlet flow rate to the chest (F_{in2}) (kg/s). A PI controller is used with controller gain

$$K_{c_h} = \frac{\tau_{I_h}}{K_{p_h}(\lambda_h + \tau_{d_h})^2}$$

and integral time constant

$$\tau_{I_h} = 2\lambda_h + \tau_{d_h}$$

The process gain between level and inlet flow rate K_{p_h} (m/kg) is

$$K_{p_h} = \frac{1}{\rho A}$$

Dilution water mixing point after LD chest

Refer to Figure A4.

It will be assumed that changes in the last dilution stream (F_{w2}) will cause the flow rate exiting the low density stock chest (F_{out2}) (kg/s) to change, but not the flow rate of the final product stream after the last dilution water mixing point (F_{prod}).

Overall material balance

$$F_{out2} = F_{prod} - F_{w2}$$

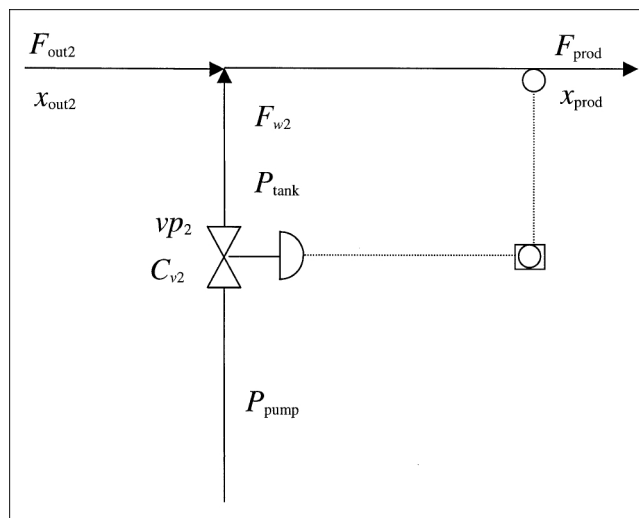


Figure A4. Dilution water mixing point after LD chest.

Flow equation

$$F_{w2} = k(vp_2/100)C_{v2}\sqrt{P_{pump} - P_{tank}}$$

The product consistency (%) x_{prod} will be controlled by manipulating the valve position vp_2 . A PI controller is used with controller gain

$$K_{c_x} = \frac{\tau_{I_x}}{K_{p_x}(\lambda_x + \tau_{d_x})}$$

and integral time constant

$$\tau_{I_x} = \tau_{p_x}$$

The consistency control valve is assumed to have first-order characteristics

$$vp_2'(s) = \left(\frac{1}{\tau_{p_x}s + 1} \right) y_2'(s)$$

Dilution header system

A linear relationship between header pressure and total dilution water flow rate is assumed

$$P_{pump} - P_{max} = \left(\frac{\bar{P}_{pump} - P_{max}}{\bar{F}_{w1a} + \bar{F}_{w1} + \bar{F}_{w2}} \right) (F_{w1a} + F_{w1} + F_{w2})$$

The dilution header system is assumed to have first-order characteristics

$$P'_{pump}(s) = \left(\frac{-P_{max}/(\bar{F}_{w1a} + \bar{F}_{w1} + \bar{F}_{w2})}{\tau_{p_p}s + 1} \right) \times [F'_{w1a}(s) + F'_{w1}(s) + F'_{w2}(s)]$$

Manuscript received Feb. 23, 1998, and revision received Apr. 1, 1999.